AD-A157 455 MEASUREMENTS OF REFRACTIVE INDEX STRUCTURE FUNCTION C2N 1/1
AND AEROSOL SIZE DISTRIBUTION AT CHESAPEAKE BAY(U)
NAVAL RESEARCH LAB WASHINGTON DC D R CUTTEN 26 JUL 85
UNCLASSIFIED NRL-MR-5593 F/G 4/1 NL

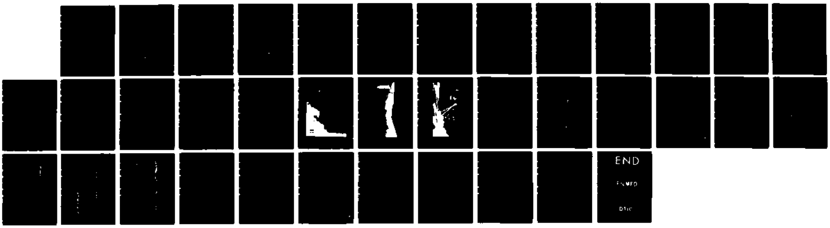

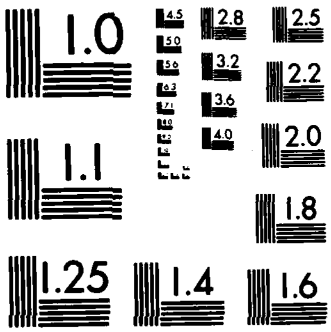
1.0
4.5
5.0
5.6
6.3
2.8
3.2
3.6
4.0
2.5
2.2
2.0
1.1
1.8
1.25
1.4
1.6

2

NRL Memorandum Report 5593

Measurements of Refractive Index Structure Function C_N^2 and Aerosol Size Distribution at Chesapeake Bay

D. R. CUTTEN

Applied Optics Branch
Optical Sciences Division

July 26, 1985

NAVAL RESEARCH LABORATORY
Washington, D.C.

Approved for public release; distribution unlimited.

SECURITY CLASSIFICATION OF THIS PAGE

REPORT DOCUMENTATION PAGE

1a REPORT SECURITY CLASSIFICATION UNCLASSIFIED	1b RESTRICTIVE MARKINGS
2a SECURITY CLASSIFICATION AUTHORITY	3 DISTRIBUTION / AVAILABILITY OF REPORT Approved for public release; distribution unlimited.
2b DECLASSIFICATION / DOWNGRADING SCHEDULE	
4 PERFORMING ORGANIZATION REPORT NUMBER(S) NRL Memorandum Report 5593	5 MONITORING ORGANIZATION REPORT NUMBER(S)
6a NAME OF PERFORMING ORGANIZATION Naval Research Laboratory 6b OFFICE SYMBOL (If applicable) Code 6530	7a NAME OF MONITORING ORGANIZATION
6c ADDRESS (City, State, and ZIP Code) Washington, DC 20375-5000	7b. ADDRESS (City, State, and ZIP Code)
8a NAME OF FUNDING / SPONSORING ORGANIZATION Naval Sea Systems Command 8b OFFICE SYMBOL (If applicable)	9 PROCUREMENT INSTRUMENT IDENTIFICATION NUMBER
8c ADDRESS (City, State, and ZIP Code) Washington, DC 20362	10 SOURCE OF FUNDING NUMBERS PROGRAM ELEMENT NO: 63754N PROJECT NO.: S0182AA TASK NO.: WORK UNIT ACCESSION NO.: 65-1812-0-5

11 TITLE (Include Security Classification)

Measurements of Refractive Index Structure Function C_N^2 and Aerosol Size Distribution at Chesapeake Bay

12 PERSONAL AUTHOR(S)

Cutten, D.R.

13a TYPE OF REPORT	13b TIME COVERED	14 DATE OF REPORT (Year, Month, Day)	15 PAGE COUNT
Interim	FROM 10/82 TO 10/83	1985 July 26	37

16 SUPPLEMENTARY NOTATION

17 COSATI CODES			18 SUBJECT TERMS (Continue on reverse if necessary and identify by block number)
FIELD	GROUP	SUB-GROUP	Optical propagation C_N
			Turbulence

19 ABSTRACT (Continue on reverse if necessary and identify by block number)

Measurements of C_N^2 using fine wire thermal probes were obtained on a 35 m tower located between the cliff face and the shoreline at Chesapeake Bay, MD. The data collected have shown, using long averaging times, that the -4/3 height dependence of C_N generally still applies in the vicinity of the cliff face with light winds coming from either over the cliff or over the water.

The aerosol size distribution data revealed very little change in the distribution with height. Over the 0.15 to 0.75μm radius range both bi-modal log-normal and power laws described the shape of the distribution curves.

20 DISTRIBUTION / AVAILABILITY OF ABSTRACT ☒ UNCLASSIFIED/UNLIMITED ☐ SAME AS RPT ☐ DTIC USERS	21 ABSTRACT SECURITY CLASSIFICATION UNCLASSIFIED
22a NAME OF RESPONSIBLE INDIVIDUAL G. L. Trusty	22b TELEPHONE (Include Area Code) (202) 767-3224 22c OFFICE SYMBOL Code 6530

DD FORM 1473, 84 MAR — 83 APR edition may be used until exhausted. All other editions are obsolete.

SECURITY CLASSIFICATION OF THIS PAGE

CONTENTS

A-1

MEASUREMENTS OF REFRACTIVE INDEX STRUCTURE FUNCTION C_N^2 AND AEROSOL SIZE DISTRIBUTION AT CHESAPEAKE BAY

1. INTRODUCTION

As a part of the US Navy's HEL program there was at the time a need to examine several sites for suitability to test high energy lasers. Any potential site needed to be characterised carefully and this would entail having meteorological, aerosol and turbulence data at the site. The Chesapeake Bay Division (CBD) of Naval Research Laboratory (NRL) was considered a potential site with its suitable topography and facilities and so would require a study of aerosol and atmospheric turbulence at the cliff face.

Therefore, the main purpose of this work was to examine the height dependence of atmospheric turbulence adjacent to the cliff face and the shoreline of the large bay. In this situation, when the wind direction is oriented towards the cliff face it could become apparent that any wind shear created may change the height dependence of C_N^2 from that which normally prevails in unstable atmospheric conditions during the daytime. Although it was intended to collect sufficient data to study the height dependence over a range of wind conditions, data collection was unfortunately restricted due to the author's return to Australia and data were only collected on four days under light wind conditions. It had also been planned to make C_N^2 measurements simultaneously from a jack-up barge located about 2 km out in the bay to obtain C_N^2 data over the water surface.

At the same time some data were also collected on aerosol size distribution as a function of height and these data are also reported.

2. EXPERIMENTAL ARRANGEMENT

A schematic layout of the location of the turbulence, aerosol and meteorological equipment at Chesapeake Bay shoreline is shown in figure 1, while figure 2 gives the location of the site on Chesapeake Bay. The equipment was located at two sites, one set at the 35 m tower and the second set on top of the cliff. The photographs in figures 3 and 4 reproduce the arrangement of the equipment on the tower carriage and at the top of the cliff. The anemometer and turbulence probes were mounted on arms about 2 m out from the tower structure to reduce any influence from it. Two aerosol spectrometer probes (PMS models ASSP-300 and CSSP-HV-100) were also attached but unfortunately the CSSP-HV-100 probe failed early in the experiment and no reliable data was obtained from it. The turbulence equipment was essentially the same system as described in reference 1 and is outlined in schematic form in figure 5. Each system consisted of a Contel MT2 unit with rms log amplifier and two probes mounted 10 cm apart on a vane assembly which held the 2 μm diameter platinum wires. The output from each amplifier was recorded on floppy discs with a HP9826 computer after the data was digitised at 2/s with an AD interfaced to the computer. Calibration of the thermal probe system was carried as described in reference 1.

Manuscript approved March 19, 1985.

As a prelude to the CBD experiment, two small experiments were conducted in the laboratory to check the performance of the thermal probe units. The first one involved comparing the output from two sets of thermal probes experiencing the same thermal fluctuations. This was done by arranging for the pairs of wires from the two sets of probes to be 20 mm apart in a horizontal plane and in the centre of a fast air flow produced by an axial fan. An example of the output from each unit is shown in figure 6 after calibration differences are removed. The results revealed very good tracking of the thermal fluctuations which was even seen out to 25 mm separation. The second experiment was set up to measure the frequency response of the thermal wires. A chopped He:Ne laser beam inpringed onto one probe wire which was suitably shielded from thermal fluctuations. The ΔT output from the Contel unit (operated in single probe mode) was used as input signal to an E G & G model 5204, lock-in amplifier whose time constant was set at 30 ms. The chopper drive was slowly scanned from 10 to 160 Hz with a sweep generator while it also provided the reference signal for the lock-in amplifier. Figure 7 shows an example of the output recorded versus sweep frequency which reveals only a drop of about -1.2 dB over the 10 to 160 Hz range. This indicates that the 2 μm platinum wires offer good frequency response up to 150 Hz. However, the HP9826 computer only allowed a maximum frequency of 1 Hz which was adequate for this work since C_N^2 data was to be averaged.

Four heights were selected on the tower to record data, namely 3, 13, 21 and 30 m. At each level data were recorded for 16 min and the carriage moved to the next level. The time lapse in changing from one level to another was generally less than 3 min.

Meteorological data recorded at the tower and cliff top included wind speed and direction, air temperature and dew point (E G & G). Data were taken between 1030 and 1600 hours although on June 20 thunderstorm activity considerably restricted the measurement period.

The site at which the tower was located consisted of a cliff line about 33 m high within 15 m of Chesapeake Bay shoreline. Vegetation covered a large part of the cliff face and the shoreline between the seawall and the base of the cliff.

3. DATA REDUCTION

3.1 Aerosol and meteorological data

The data recorded on tape at 1 s intervals with the NRL mobile van facility were reduced to produce data of 10 min average in the standard NRL format(ref.2). From this format the data can be sorted and plotted at appropriate intervals. For this analysis a 10 min average was selected; chosen as it is the closest to the 16 min interval used to record the turbulence data.

3.2 Turbulence data

The refractive index fluctuations can be described by a structure function:

$$D_n(\bar{r}) = [n(\bar{x}) - n(\bar{x}+\bar{r})]^2$$

where $\bar{r}$ is the displacement vector between two points in space. A similar structure function can be defined for temperature $D_T(\bar{r})$. Assuming locally isotropic and homogeneous turbulence, Kolmogorov[1] derived a structure function in the form:

$$D_n(r) = C_N r^{2/3} \quad \text{and} \quad D_T(r) = C_T r^{2/3} = \Delta T^2 r^{2/3}$$

where $l_o < r = |\bar{r}| < L_o$ defines the limits of the sub-inertial range, and C_N and C_T are the structure - function parameters for refractive index and temperature. The expression which relates C_N^2 to temperature fluctuations is given by:

$$C_N^2 = (2627\text{x}10^{-6} P/T^2)^2 \left(\frac{\Delta T_{rms}}{r^{1/3}}\right)^2 \qquad (1)$$

where T is the air temperature (K), P is the atmospheric pressure (in Hg) and r is the probe separation (cm). The C_N^2 data were recorded over a 16 min period at a particular level on the tower and on the cliff top, simultaneously.

The simultaneous recordings were plotted together on the one plot. Figures 8 to 13 reproduce six of the ten sequences of data recorded at each of the 4 levels on the tower. The left hand scale of the plots is the voltage output from the RMS logarithmic amplifier while the right hand scale gives the C_N^2 values calculated from the voltage fluctuations using equation (1) since $\Delta T_{RMS} = \Delta V_{RMS}/\alpha K$ where K is the calibration constant and α is the thermo-resistive coefficient for Pt wire(ref.1). Included on the plots are the mean C_N^2 and standard deviation values for the voltage fluctuations. Since the calibration factors for the two probe systems were different a correction factor was added to the logarithm of the voltage before plotting, from the unit located at the cliff top. This allows C_N^2 data for the two sites to be compared directly. The 16 min average used can generally be regarded as a sufficiently long time to reduce differences arising from time-averages and ensemble-averages of the C_N^2 parameter. Hence, it is expected that changes in C_N^2 with time would be smooth.

4. TURBULENCE ANALYSIS

4.1 Height dependence of C_N^2

One of the main purposes of this turbulence data analysis was to examine the height dependence of C_N^2. The semi-empirical theory drived by Wyngaard and Izumi(ref.3) gave a vertical profile of C_N^2 as:

$$C_T^2 \approx \tfrac{4}{3}(-Q/u_*)^2(-L)^{2/3} z^{-4/3} \qquad (2)$$

where Q = surface temperature flux ($^{\circ}C\ cmS^{-1}$)

u_* = kinematic surface stress (stress per unit air density exerted by the wind on the surface)

L = Monin-Obukhov length

Z = height

This expression really only provides a profile of C_T^2 when $-7Z/L >> 1$ and therefore only applies after the first few metres. For sunny days with light winds, $L \approx 10$ m and hence the above criteria will apply above several metres. It should be noted equation (2) derivation is for very unstable conditions which generally occur during the day when heat transfer is upward and $Z/L < 0$. For light winds, μ_* is generally very small under unstable conditions and a free convection situation is approached but never realised. Typically, μ_* is about an order of magnitude smaller than the local wind speed. Under stable conditions (eg night time) C_T^2 decreases with height more slowly than $Z^{-2/3}$. It should be remembered that equation (1) which relates C_T^2 to C_N^2 does not take into account the effects of water vapour fluctuations which would contribute to optical turbulence. The data presented in this paper are examined to see if the form of equation (2) still applies in the vicinity of a high cliff located adjacent to a shoreline where wind shear could be expected to be present. It is also possible the surface heat transfer could become highly variable at the shoreline although it is expected not to have had sufficient time to do so if the air has come from over the water.

4.2 Results

Four days of data taken in June 1983 have been examined. Generally clear, sunny conditions were experienced with winds less than 4 m/s. On all except one day the wind direction was from over the water. The data have been sorted into 10 groups which represent either a single ascent or descent on the tower. For each group C_N^2 was recorded for 16 min at each of four levels and averaged. These data have been plotted in figure 14 and a linear least squares regression fit was performed on each group. The results are summarised in Table 1 where the slope m and the regression coefficient are listed. The values of m range between 1.13 and 2.16 with a coefficient of regression better than 0.957 in all except one case. The range of values of m indicate that the exponent in the height expression for the long term averaged C_N^2 data fall within a defined region around $m = 4/3$. Excluding the June 17 value for reasons given below, the mean value of m derived from the 9 values was 1.43 with a standard deviation of 0.21. Equation (2) which provides $Z^{-4/3}$ dependence of C_N^2 only when there is strong illumination and low values of wind speed (the conditions most applicable to the measurements made at Chesapeake Bay, ie well-developed unstable atmosphere near the surface) is thus generally supported.

In contrast, the Atmospheric Sciences Laboratory data given in reference 4 and reproduced in Table 2 shows that the exponent has a much broader range of variability. In this experiment C_N^2 was recorded at each of the 3 levels on a tower in the desert for a period of 10 s. With a large standard deviation experienced in C_N^2 for a desert terrain, this could be expected to happen. If one looks at the C_N^2 data for CBD site in figures 8, 10 and 12, periods exist where C_N^2 for the higher levels is considerably lower than the mean C_N^2 value. These periods appear to last for up to 30 s and if they do not occur simultaneously at each level on the recording tower then one can expect large variation in the slope of the C_N^2 versus Z plot, ie the short-term averages of C_N^2 would give a very ragged profile.

Therefore it would appear that the -4/3 dependence on Z holds better for the situation where C_N^2 has been averaged over long periods (~16 min) rather than very short periods where one is virtually dealing with instantaneous changes in C_N^2. The one exception to this was on June 17 1983, where long periods of very low turbulence were recorded at the top 2 recording levels of the tower resulting in very low voltages and consequently a higher error is implied.

The standard deviation (σ) for the rms log amplifier output from the probe unit at the tower are listed in Table 3. It can be generally concluded that no obvious trend of σ with height is observable except on June 17 where it appears that σ does drop with height. On June 23 σ at the 3 m level was at least double that at all other levels which is presumably due to the very low wind speed occurring.

The C_N^2 data recorded at the cliff top for 3 different days has been plotted in figure 15 as a mean of the 16 min recording period along with the standard deviation and wind speed. These data do not reveal any significant phenomena occurring in C_N^2. The average value begins to fall off after about 1400 hours when the solar heating of the ground is beginning to drop; this occurring later than midday due to daylight saving time. There appears to be no dependence of C_N^2 on wind speed and there were no substantial shifts in wind direction on a particular day.

Table 4 gives the comparisons of mean C_N^2 calculated from 16 min averages at cliff top and at the 3 m level on the tower. Note that these recordings of C_N^2 were made simultaneously. On 3 of the 4 days the mean C_N^2 values at the two sites are very similar. However, on June 23, the mean C_N^2 at the tower is up to an order of magnitude lower than at the cliff top. On this day the average wind speed over the 16 min recording periods at both sites was less than 0.9 m/s. It is also noteworthy that the standard deviation σ for log amplifier output voltage at the 3 m level is at least double that for the cliff top. On previous days values of σ for the two sites were similar.

With such limited data it is difficult to speculate as to why such a large difference in C_N^2 occurred on this day. The larger σ value could account for a lower than usual value of C_N^2 at the 3 m tower level. Very light winds may not have mixed the cooler air coming from over the water which results in macro-scale turbulence occurring at the shoreline.

5. AEROSOL SIZE DISTRIBUTION ANALYSIS

The analysis of the aerosol size distributions was unfortunately restricted to only one probe providing reliable data. Even so, some curve fitting was attempted to the size distribution data in the size range 0.15 to 0.75 µm radius. Again, only data from four days are examined. The curves represent a 10 min average of 1 s data which fell within the 16 min interval when the carriage was at a particular level on the tower. Figures 16 to 19 show a sample of plots on each of the days data were measured. The plots also give the average meteorology parameters for the 10 min period. On three of these days (June 17, 20 and 23) the plots exhibit a bimodal distribution with the first mode located somewhere below 0.15 µm and the second one near 0.5 µm. Wind direction on these days was from over the water so it is not unexpected to find a bimodal distribution. On the other day (June 22) a power law distribution is more applicable. The wind on this day was from W to NW which would imply a rural/urban composition.

For the bimodal data a log-normal curve with two components was used to provide the number density per unit radius as follows:

$$n(r) = \frac{dN(r)}{dr} = \sum_{i=1}^{2} \left(\frac{N_i}{2.303 \; r\sigma_i \sqrt{2\pi}} \right) \exp\left(- \frac{(\log \; r/r_i)^2}{2\sigma_i^2} \right) \qquad (3)$$

where σ = standard deviation

r_i = mode radius

N_i = number density with r_i

The power law distribution used was of the form:

$$n(r) = \frac{dN(r)}{dr} = A \; r^{-k} \qquad (4)$$

where A and k are constants.

The bimodal curves were fitted to the data by eye while the power law curves were fitted by linear regression. The parameters used for the curve fitting are detailed in Tables 5 to 8. For bimodal curve fitting it has been assumed that the mode radius for the smaller particles is 0.03 μm which is generally what is observed for continental component.

The bimodal curve fit to the data measured on June 17 shows a decreasing trend in the standard deviation of the larger particle component with increasing wind speed after 1440 hours at the 13 m level. It would appear that the range of larger particles has been narrowed slightly as the wind speed was doubled. The smaller particle component did not appear to be affected although the number density (N_1) did rise when W_s increased. For the June 23 data where bimodal, log-normal curve fits were also done, the parameters did not show any significant trend. The calculated number density (N_1) at the mode radius r_1 did reveal some variability with a possibility slightly lower value at the 3 m and 13 m levels.

The appropriate curve fit to the aerosol size distribution data on June 22 was a power law curve. There was a negligible change in the exponent value over the total period where the wind speed was reasonably steady while there was a drop in the coefficient A which would signify a decrease in the number density (see Table 8). The reason for such a curve fit being a power law was possibly because the air mass was from over the land and nearby Washington urban area.

The bimodal distribution mode radii for the larger particles given in Tables 5 and 7 do fall closely to those used for the LOWTRAN 5 rural and urban aerosol distribution model although the standard deviation is up to half that used for those models(ref.5). The assumption of $r_1 \approx 0.03$ μm as the mode radius for the small continental particles seemed reasonable. The mode radii given in reference 5 are for moderate humidities of 70 to 80%. Humidities in the range of 45 to 85% prevailed while the aerosol size measurements were made.

6. CONCLUSIONS

Although only a limited amount of turbulence and aerosol size distribution data were available for analysis some conclusions can be drawn. These are summarised as follows:

6.1 Turbulence

(1) For long averaging periods, C_N^2 measured near the cliff face has an inverse law dependence on height: the exponent taking values which are near -4/3 as predicted by the theory for unstable conditions in light winds. Wind direction did not appear to influence the height dependence. Hence, one can conclude that the wind flow properties do not appear to be all that drastically altered at the shoreline.

(2) Recordings of turbulence made a few metres above the ground showed clearly that long averaging times are needed to minimise differences between time and ensemble averages.

(3) Averaged C_N^2 measured at the cliff top and at the base of the tower were on most times similar indicating little influence on C_N^2 from wind and topography.

6.2 Aerosol size distribution

(1) Little change was observed in the shape of the size distribution curve with height on a particular day.

(2) Two types of distributions were observed to occur, namely bimodal log-normal and power law, depending on the direction of the wind. This switching in distribution shapes may be due to the close proximity of the site to a large urban environment.

7. ACKNOWLEDGMENTS

This work was carried out while the author was attached to NRL as a TTCP exchange scientist and is indebted to the assistance of Tom Cosden and John Cox in mounting the instrumentation on the tower.

TABLE 1. SUMMARY OF THE VALUES DETERMINED FOR m IN THE HEIGHT DEPENDENCE OF C_N^2 AT CBD SHORELINE

Date	Ascending or Descending	Time Period (EDT)	m	r^2	Ave W_S (m/s)	Ave W_D (deg)
June 16	D	1416-1545	-1.32	0.61	3.0	150
June 17	D	1213-1340	-2.16	0.961	1.3	142
June 22	A	1059-1230	-1.72	0.970	3.6	315
	D	1213-1336	-1.66	0.997	3.6	320
	A	1319-1443	-1.56	0.998	3.5	335
	D	1425-1548	-1.34	0.990	3.1	330
June 23	A	1034-1158	-1.27	0.957	1.1	43
	D	1140-1259	-1.13	0.975	1.2	48
	A	1242-1359	-1.26	0.970	0.6	71
	D	1342-1510	-1.63	0.948	0.7	100

TABLE 2. SUMMARY OF m AND r^2 VALUES FROM FITS TO WSMR C_N^2 DATA TAKEN AT 8,15 AND 32 M HEIGHTS USING 10 S RECORDS

Day	Time	m	r^2
289	0845	-1.80	0.92
	0928	-1.39	0.85
	1720	-5.17	0.97
	1750	-4.82	0.94
	1818	-0.48	0.19
	1832	-1.73	0.24
290	1731	-0.58	0.95
	1758	-1.62	0.97
	1828	-2.73	0.99
	1840	-2.31	0.98

NB. Data taken from reference 4.

TABLE 3. STANDARD DEVIATION VALUES FOR C_N^2 PROBE VOLTAGE AT THE TOWER

Day	Height (m)	σ	Day	Height (m)	σ
June 16	13	0.37	June 22	30	0.68
	21	0.39		21	0.67
	30	0.74		13	0.81
				3	0.60
June 17	30	0.37			
	21	0.44	June 23	3	1.47
	13	0.58		13	0.73
	3	1.22		21	0.72
				30	0.75
June 22	3	0.65		21	0.57
	13	0.77		13	0.65
	21	0.62		3	1.49
	30	0.57		13	0.79
	21	0.77		21	0.75
	13	0.73		30	0.57
	3	0.62		21	0.77
	13	0.76		13	0.76
	21	0.66		3	1.51

TABLE 4. COMPARISON OF C_N^2 MEASURED AT THE BASE OF THE TOWER AND AT THE CLIFF TOP ON FOUR DAYS.

Day	Time	C_N^2 (Tower)	C_N^2 (Cliff Top)	Tower W_S	Tower W_D	Cliff Top W_S	Cliff Top W_D
June 17	1323	1.35×10^{-13}	1.53×10^{-13}	0.9	145	1.1	70
June 20	1126	1.94×10^{-14}	4.22×10^{-14}	2.0	285	0.9	240
June 22	1100	9.3×10^{-14}	1.11×10^{-13}	2.4	267	1.5	270
	1319	6.94×10^{-14}	5.72×10^{-14}	3.2	315	1.5	285
	1530	3.88×10^{-14}	5.05×10^{-14}	2.8	315	1.3	290
June 23	1034	3.45×10^{-14}	2.65×10^{-13}	0.7	80	0.8	105
	1242	2.54×10^{-14}	2.54×10^{-13}	0.8	60	0.6	115
	1443	5.53×10^{-14}	1.42×10^{-13}	0.8	115	0.7	135
	1502	4.02×10^{-14}	1.22×10^{-13}	0.1	100	0.7	120

TABLE 5. COEFFICIENTS FOR BIMODAL LOG-NORMAL FIT TO AEROSOL SIZE DISTRIBUTION DATA MEASURED ON JUNE 17 1983 AT CBD SHORELINE

Height (m)	Time	N1	r_1 (μm)	r_2 (μm)	σ_1	σ_2	W_S (m/s)	W_D (deg)
30	1240	1.4×10^5					1.4	139
21	1300	1.2×10^5					1.6	143
13	1320	1.2×10^5	0.03	0.5	0.25	0.20	1.2	144
3	1340	1.1×10^5					0.8	144
13	1400	1.2×10^5					1.6	154
13	1420	5.3×10^5	0.03	0.5	0.22	0.20	2.3	153
13	1440	3.8×10^5	0.03	0.5	0.22	0.20	3.0	154
13	1500	4.9×10^5	0.03	0.5	0.22	0.15	3.0	156
13	1520	2.7×10^5	0.03	0.5	0.225	0.15	3.8	157
13	1540	1.3×10^5	0.03	0.5	0.225	0.10	4.1	155

TABLE 6. COEFFICIENTS FOR BIMODAL LOG-NORMAL FIT TO AEROSOL SIZE DISTRIBUTION DATA MEASURED ON JUNE 20 1983 AT CBD SHORELINE

Height (m)	Time	N_1	r_1 (μm)	r_2 (μm)	σ_1	σ_2	W_S (m/s)	W_D (deg)
3	1120	5.0×10^3	0.03		0.225		0.1	108
13	1130	7.5×10^3	0.03	0.4	0.225	0.2	1.0	233
13	1140	7.5×10^3	0.03	0.4	0.225	0.2	3.0	333

TABLE 7. COEFFICIENTS FOR BIMODAL LOG-NORMAL FIT TO AEROSOL SIZE DISTRIBUTION DATA MEASURED ON JUNE 23 1983 AT CBD SHORELINE

Height (m)	Time	N1	r_1 (μm)	r_2 (μm)	σ_1	σ_2	W_S (m/s)	W_D (deg)
3	1100	2.7×10^5	0.03	0.4	0.2	0.2	0.6	64
13	1120	2.3×10^5					1.2	30
21	1140	2.4×10^5	0.03	0.4	0.2	0.15	1.1	37
30	1200	2.1×10^5					1.5	29
21	1220	1.1×10^5	0.03	0.4	0.2	0.2	1.2	31
13	1240	5.9×10^4					0.9	45
3	1300	5.9×10^4	0.03	0.5	0.25	0.15	0.8	51
13	1320	5.9×10^4					0.6	49
21	1340	2.2×10^5					0.5	95
30	1400	1.5×10^5					0.6	83
21	1420	1.2×10^5	0.03	0.4	0.2	0.15	0.6	67
13	1440	8.1×10^4					0.9	115
3	1500	8.9×10^4					0.7	114

TABLE 8. COEFFICIENTS FOR POWER LAW FIT TO AEROSOL SIZE DISTRIBUTION DATA MEASURED ON JUNE 22ND 1983 AT CBD SHORELINE

Height (m)	Time	A	k	W_S (m/s)	W_D (deg)
13	1130			3.2	331
21	1200			3.4	350
30	1230	9.33	-3.56	3.5	325
13	1300			3.9	342
3	1330			2.6	298
13	1400			3.8	340
30	1430	4.47	-3.55	3.9	347
21	1500			3.0	342
13	1530			3.5	336

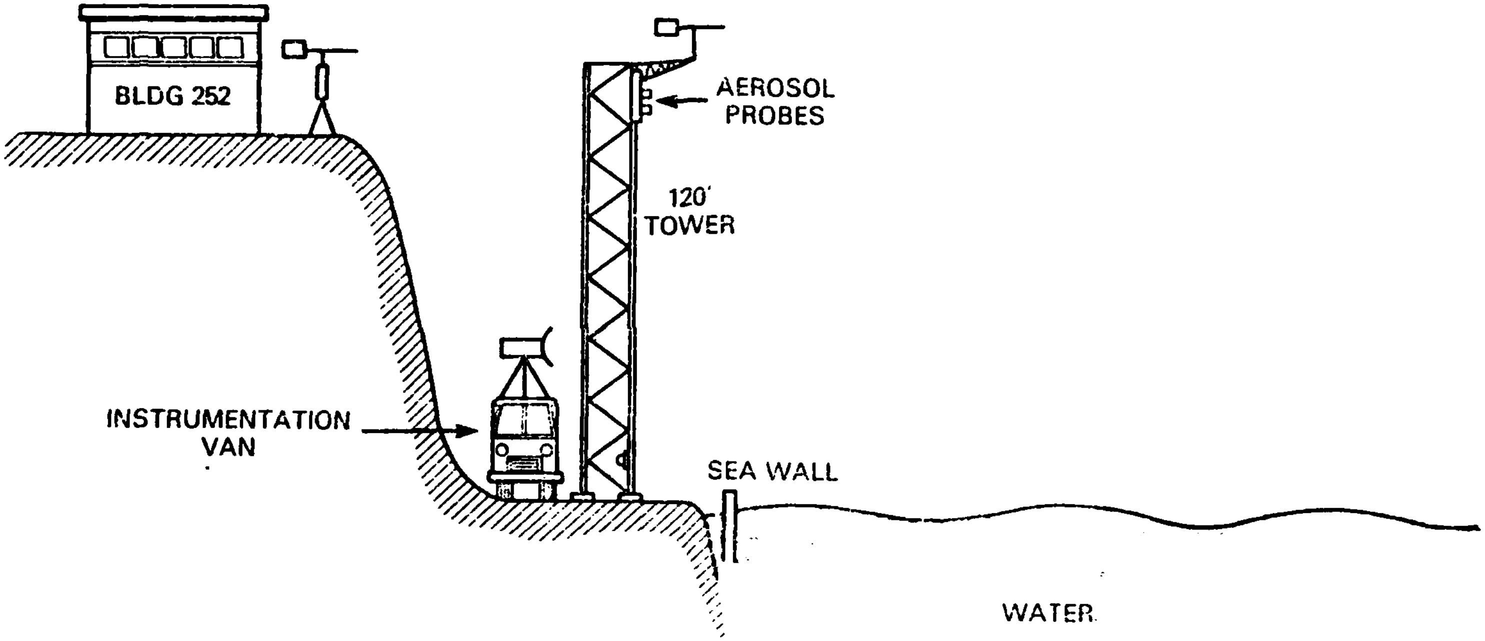

Fig. 1 — Schematic of the typography at the measuring site

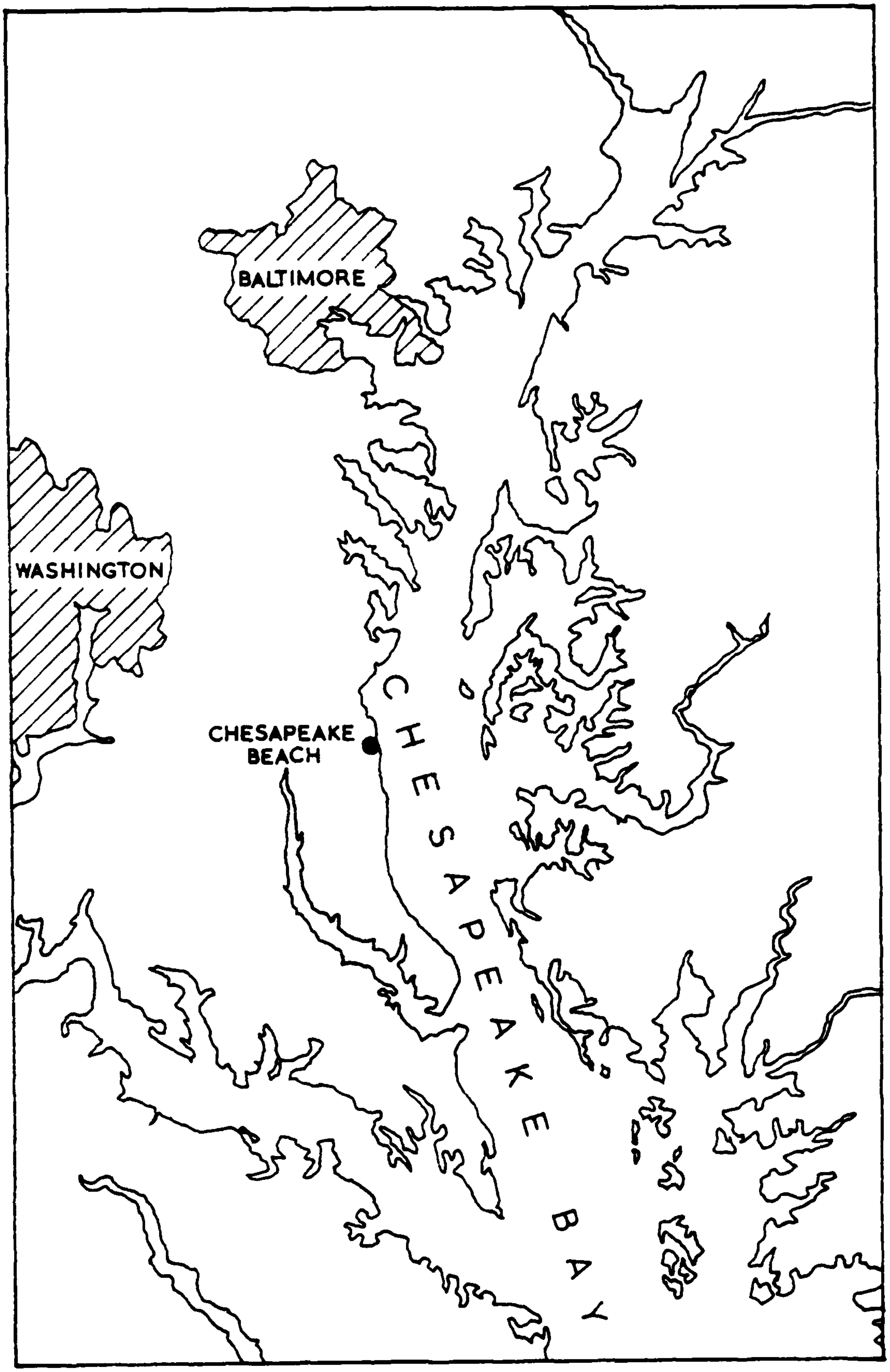

Fig. 2 — Schematic showing location of measuring site on Chesapeake Bay

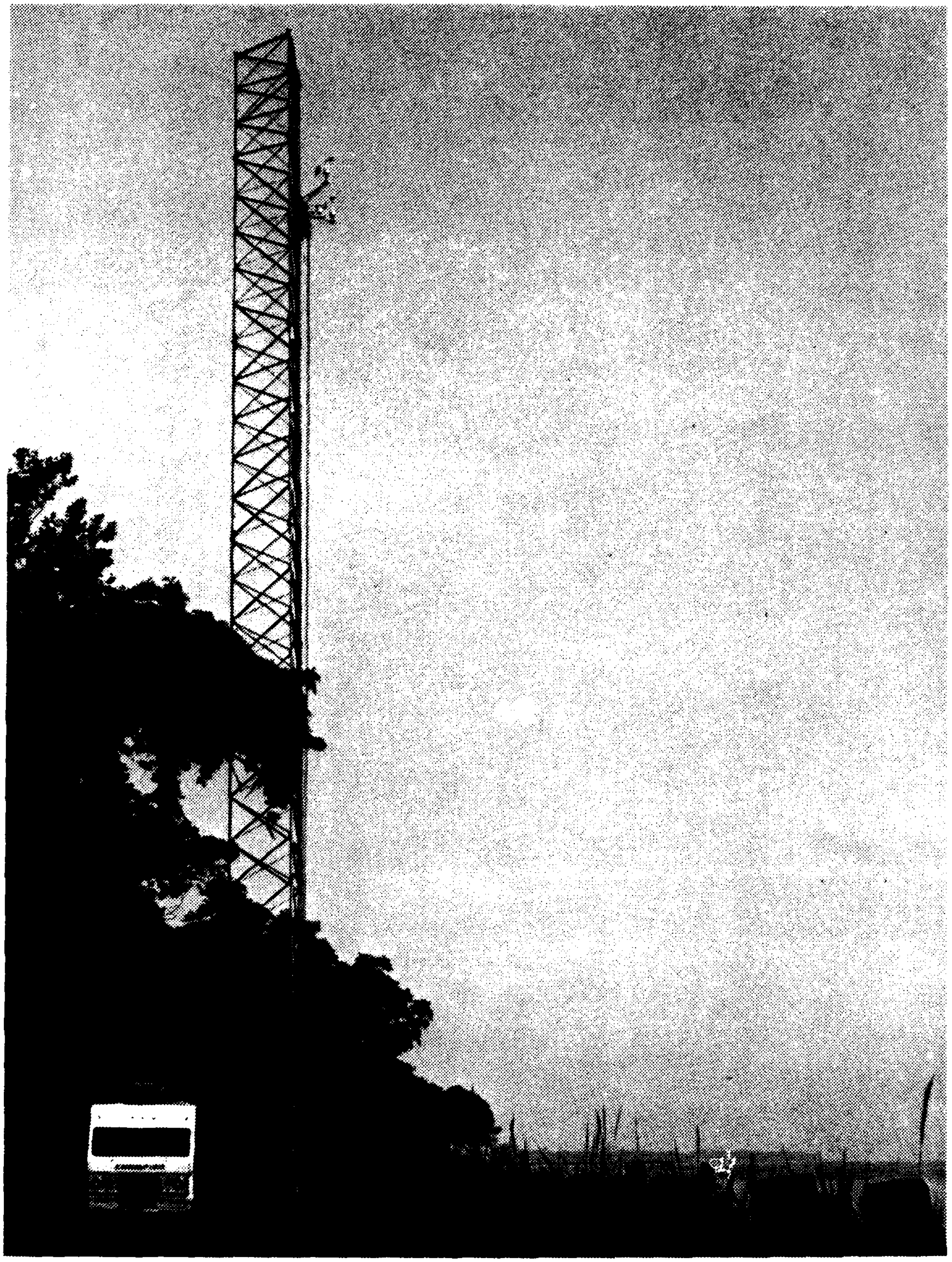

R-1140

Fig. 3(a) — Photograph showing the 35 m tower on the shoreline

R-1141

Fig. 3(b) — Photograph showing a view from the top of the cliff face

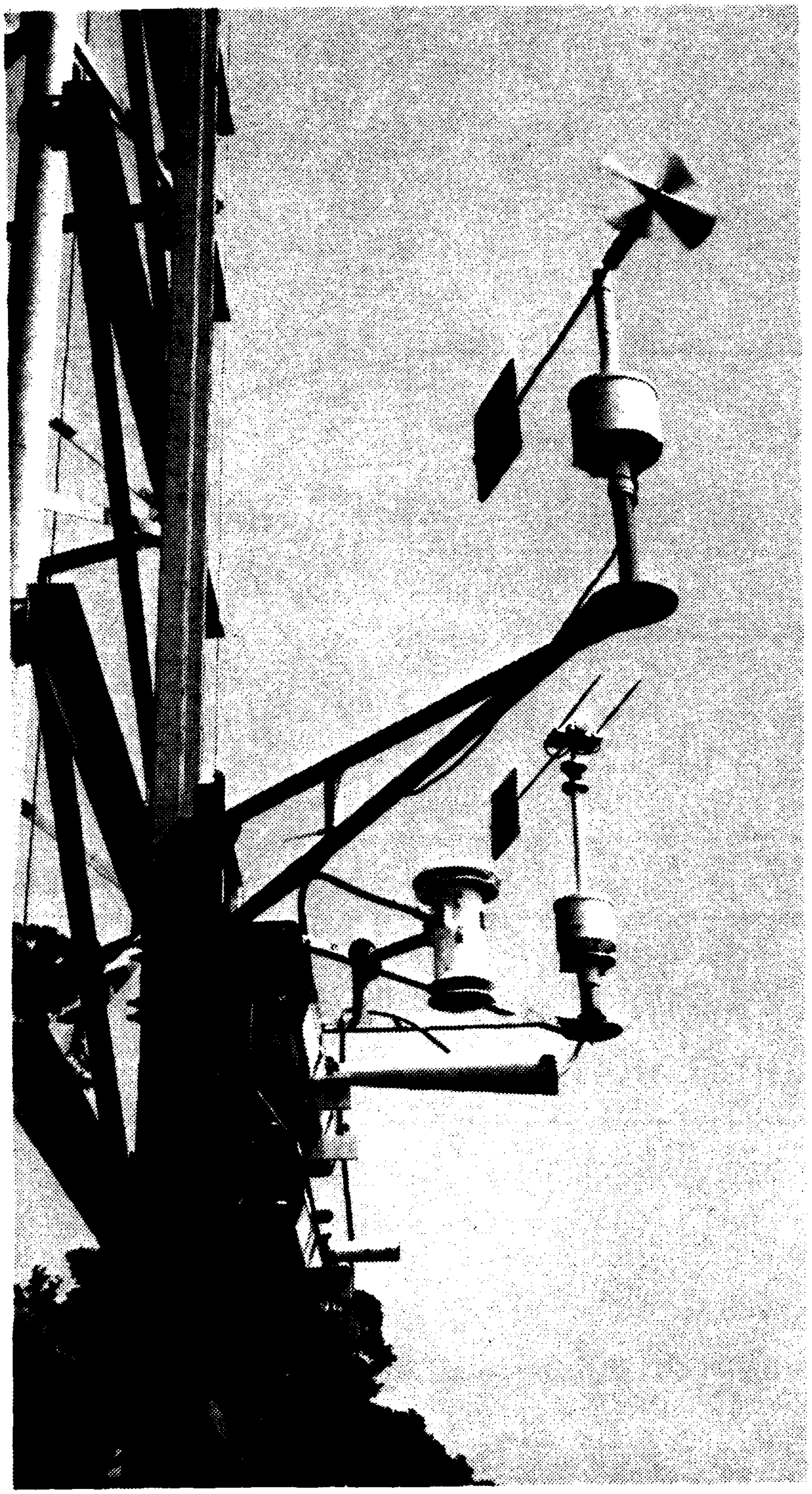

R-1142

Fig. 4 — Photograph of the instrumentation attached to the carriage on the tower

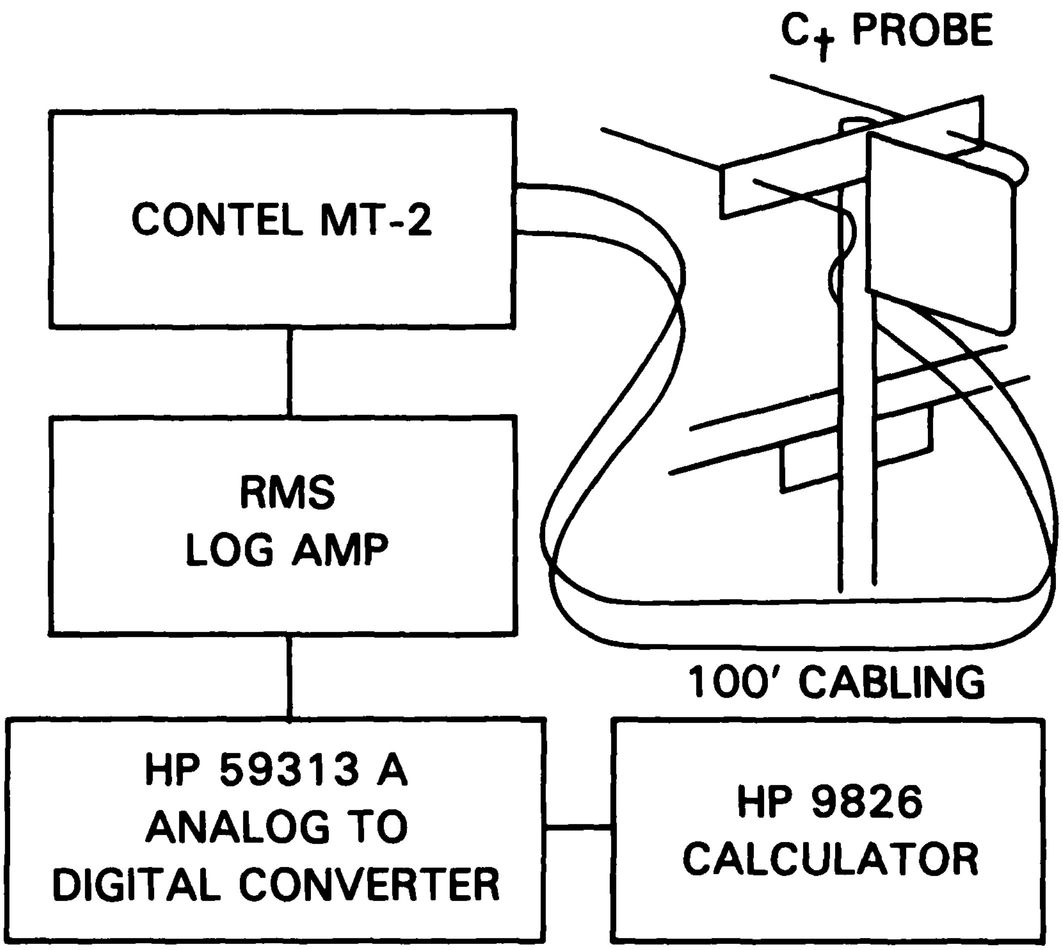

Fig. 5 — A schematic of the micro-thermal double probe system

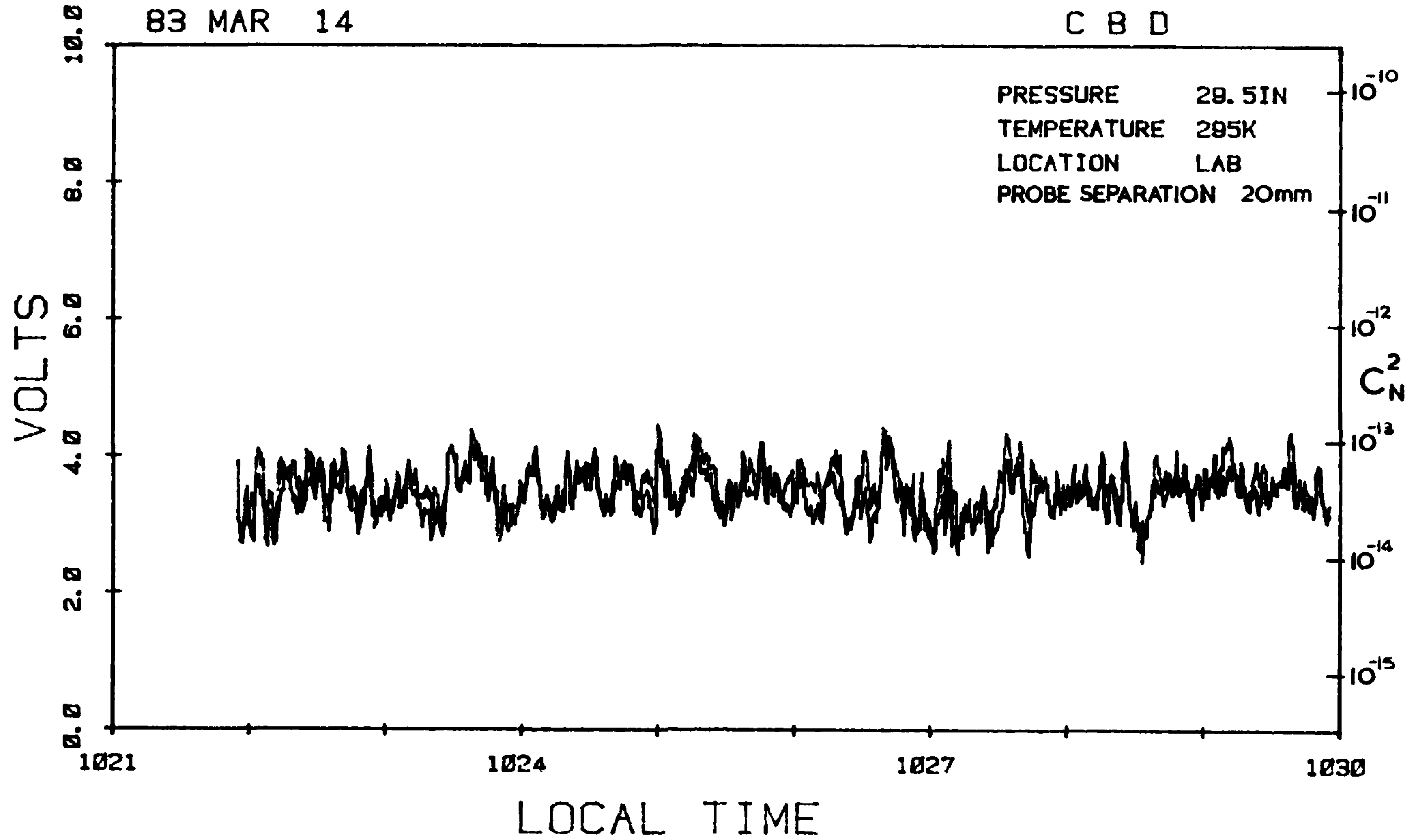

Fig. 6 — Comparison of the output voltage from two microprobe systems sampling the same thermal fluctuations

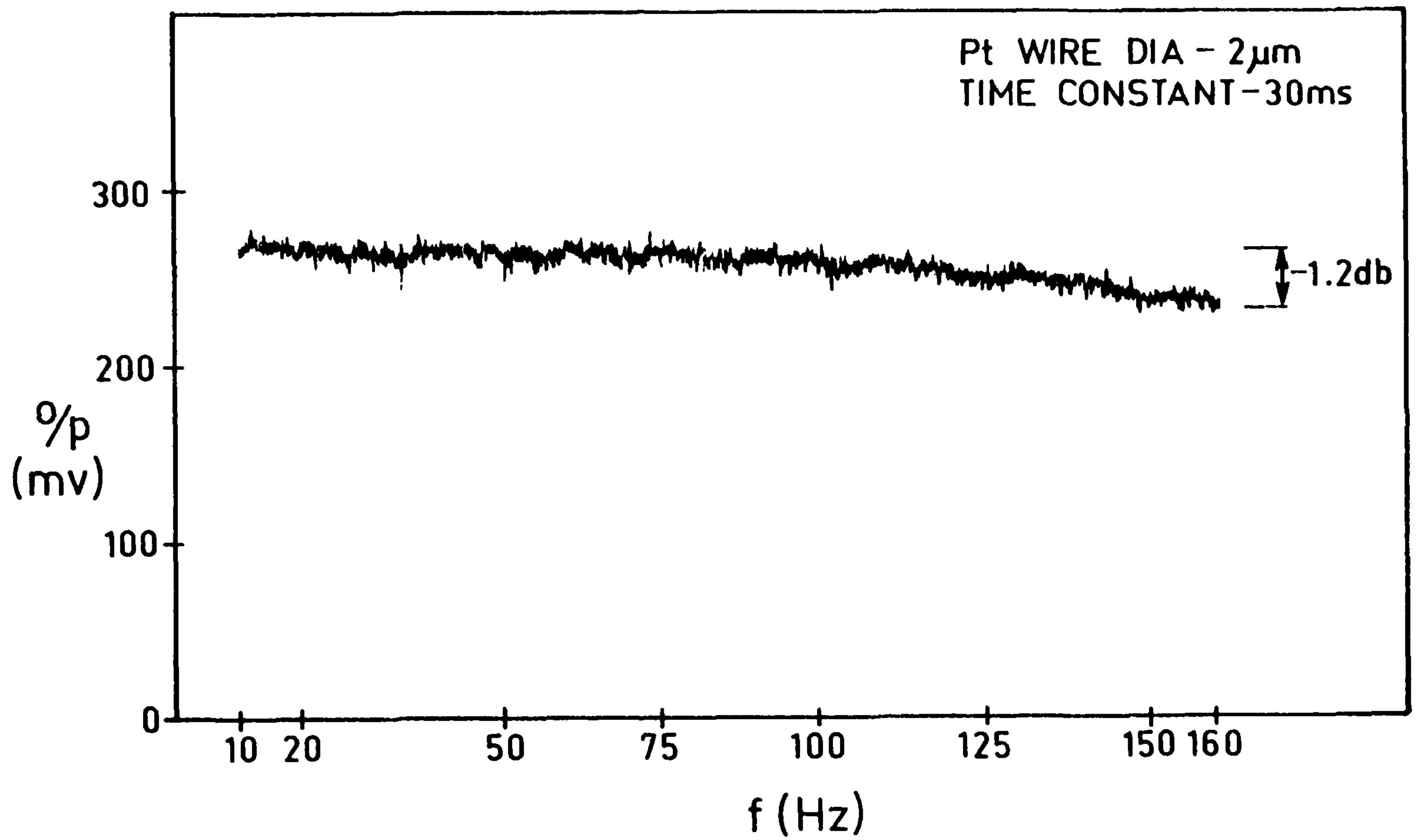

Fig. 7 — Frequency response of the micro-thermal probe system

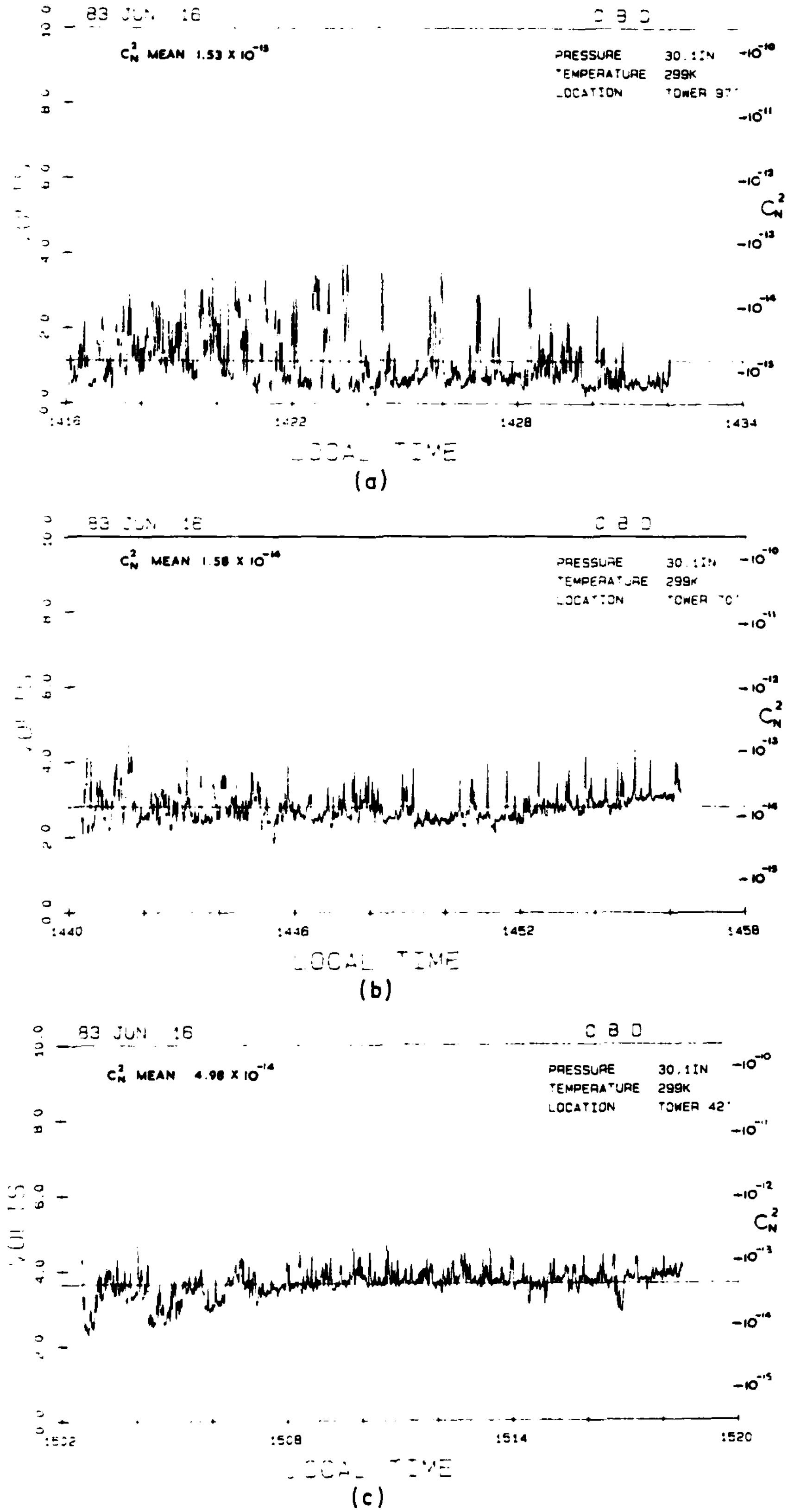

Fig. 8 — C_N^2 recordings made on the tower for June 1983

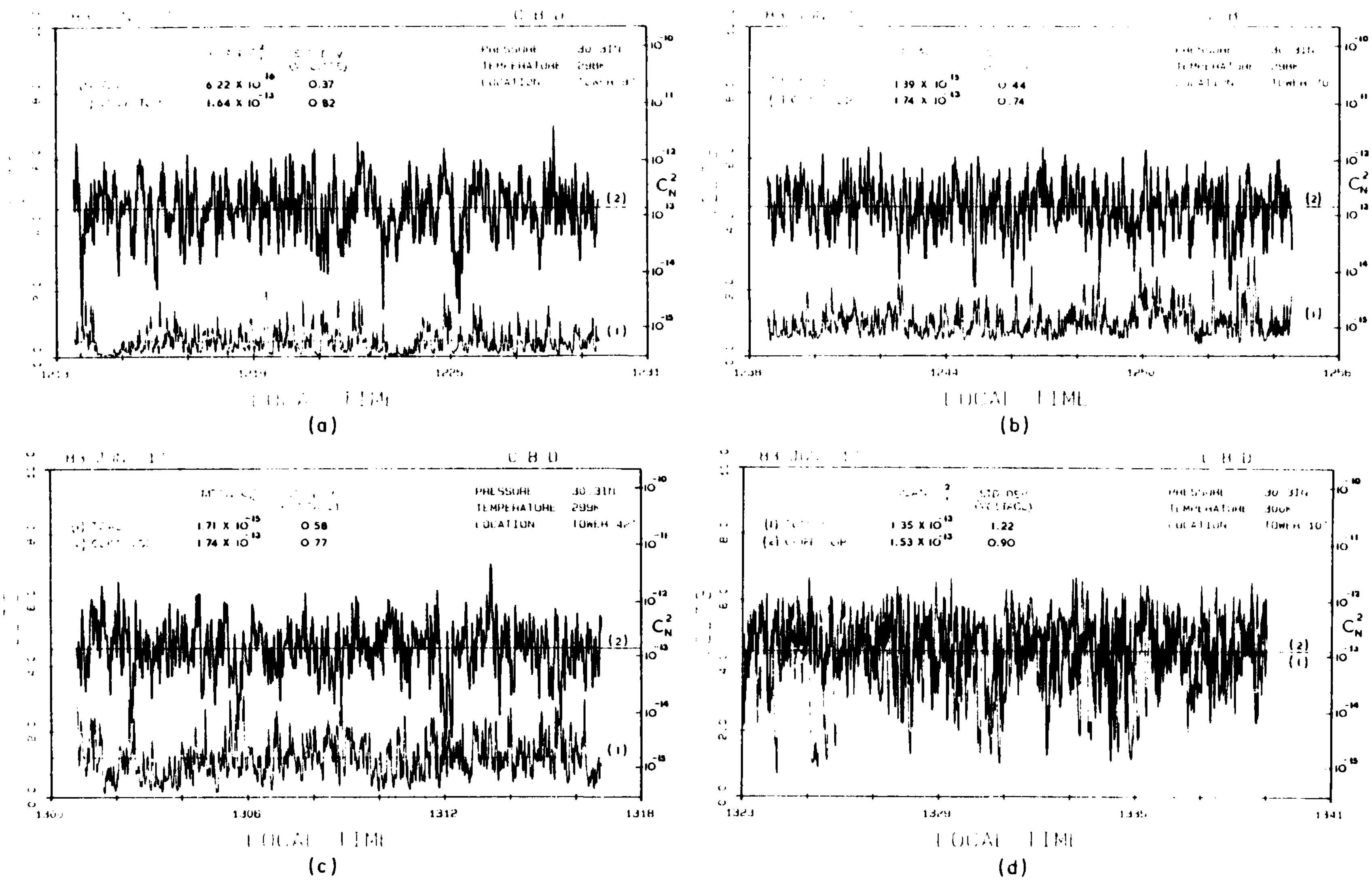

Fig. 9 — C_N^2 recordings made at each level on the tower and cliff top for June 17 1983

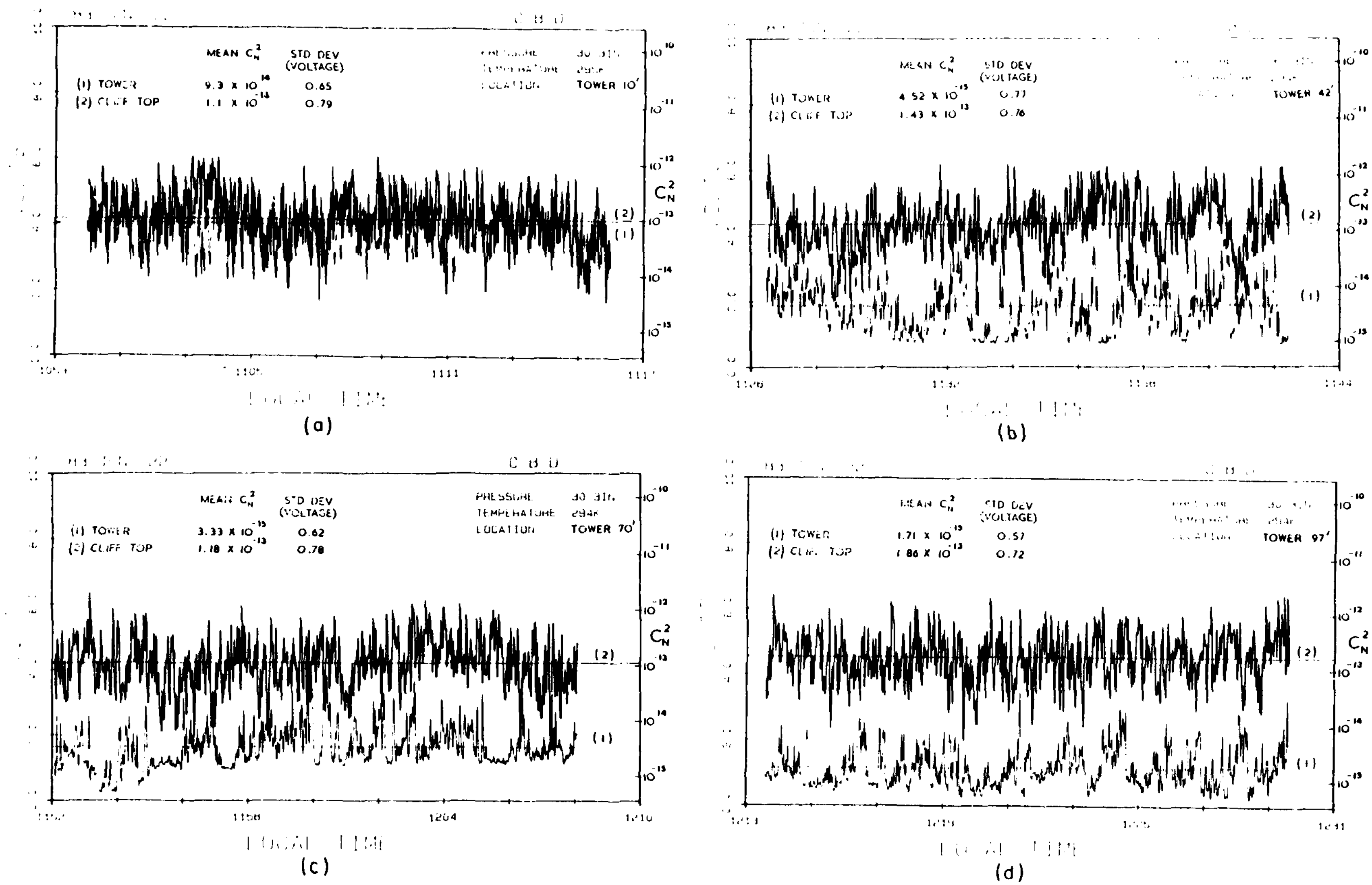

Fig. 10 — C_N^2 recordings made at each level on the tower and cliff top between 1100 and 1230 EDT on June 22 1983

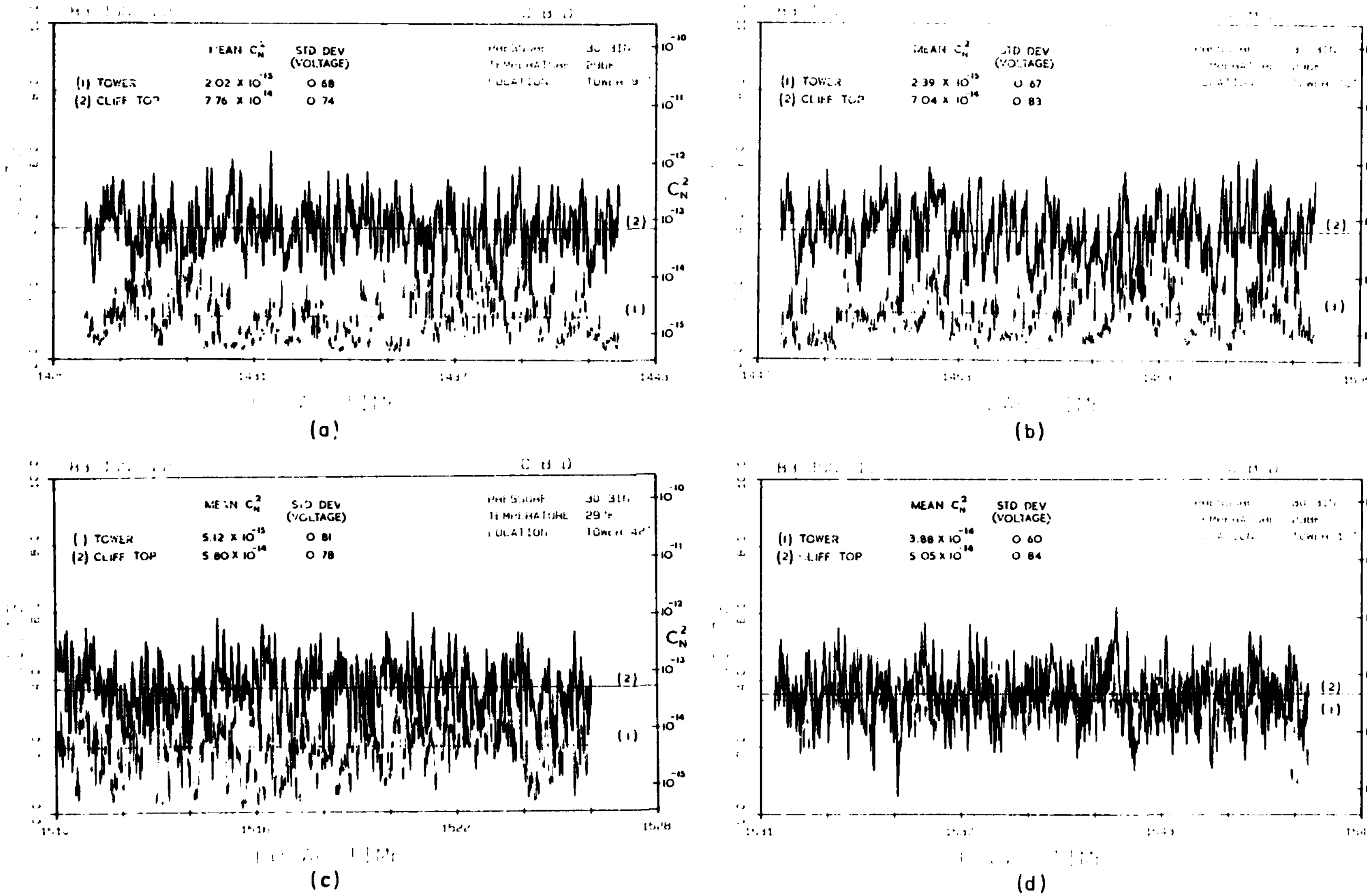

Fig. 11 — C_N^2 recordings made at each level on the tower and cliff top between 1425 and 1548 EDT on June 22 1983

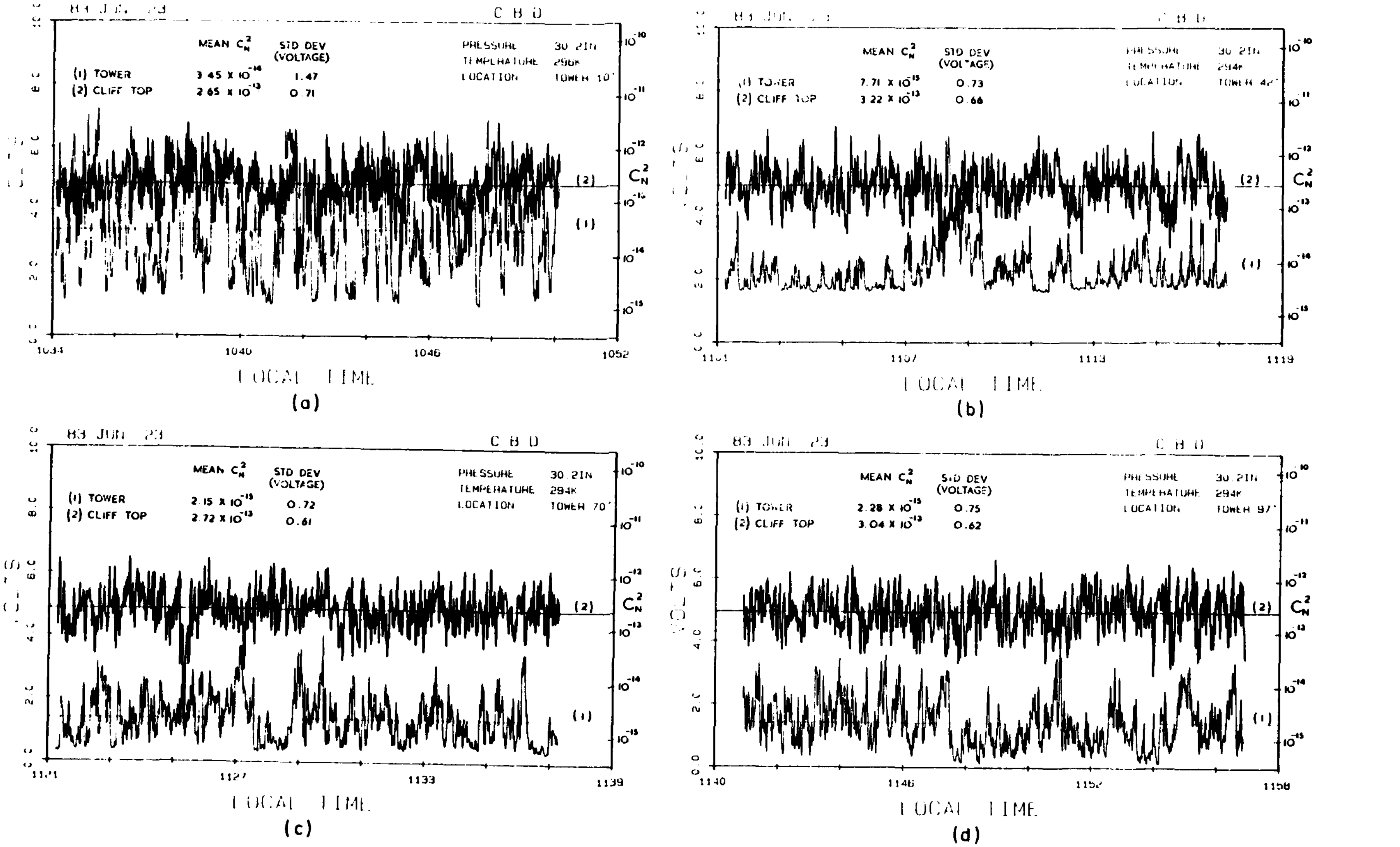

Fig. 12 — C_N^2 recordings made at each level on the tower and cliff top between 1034 and 1157 EDT on June 23 1983

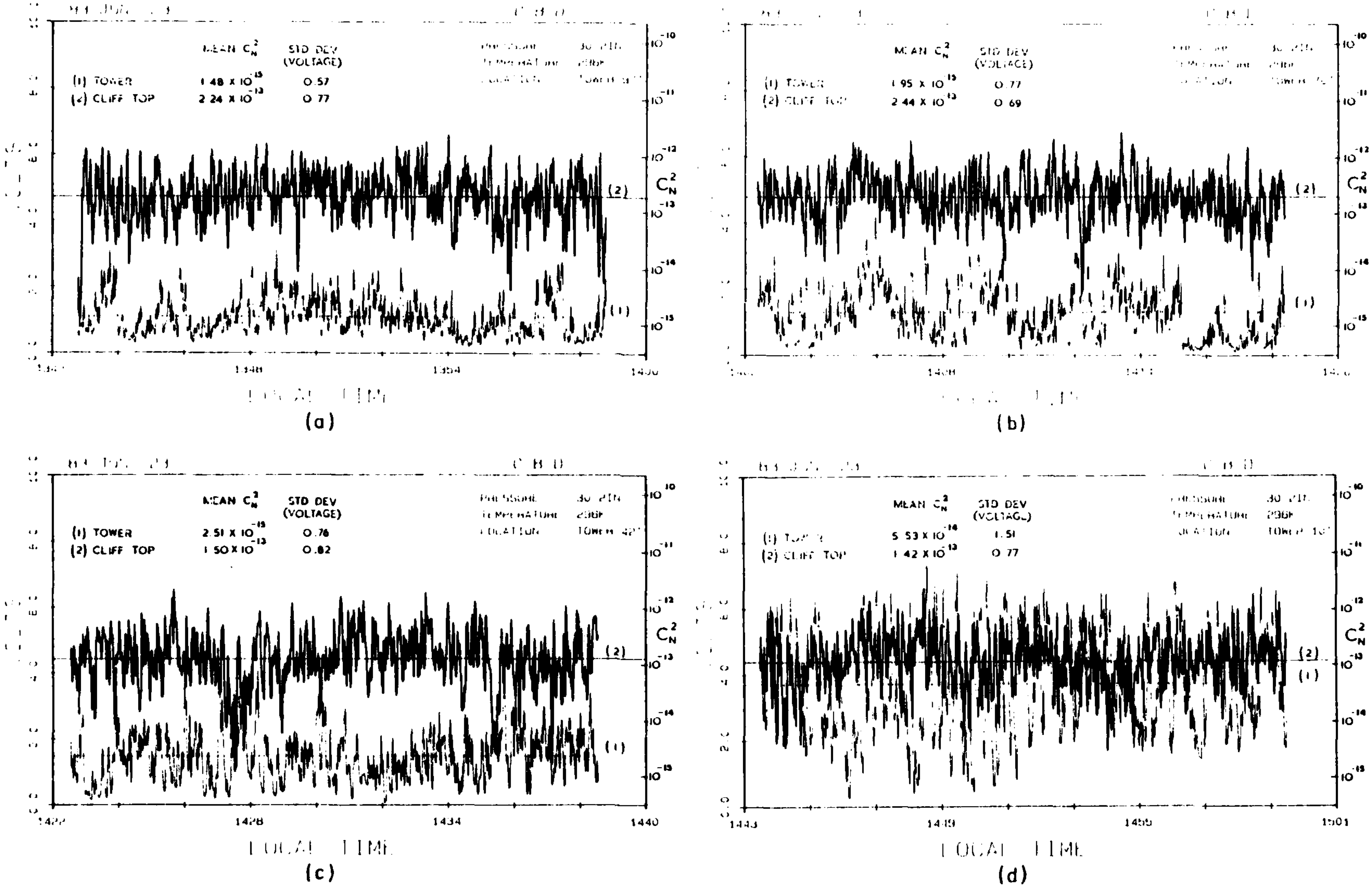

Fig. 13 — C_N^2 recordings made at each level on the tower and cliff top between 1342 and 1500 EDT on June 23 1983

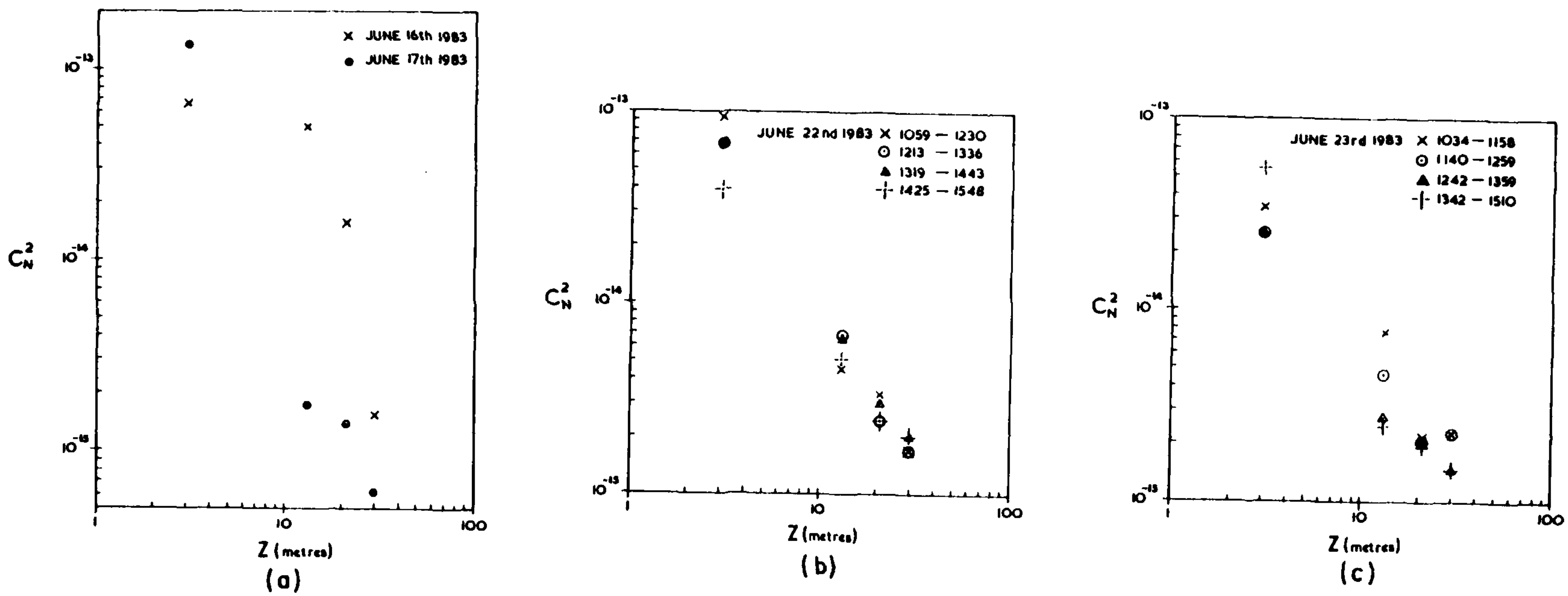

Fig. 14 — Plots of C_N^2 versus height for data measured at CBD on four days

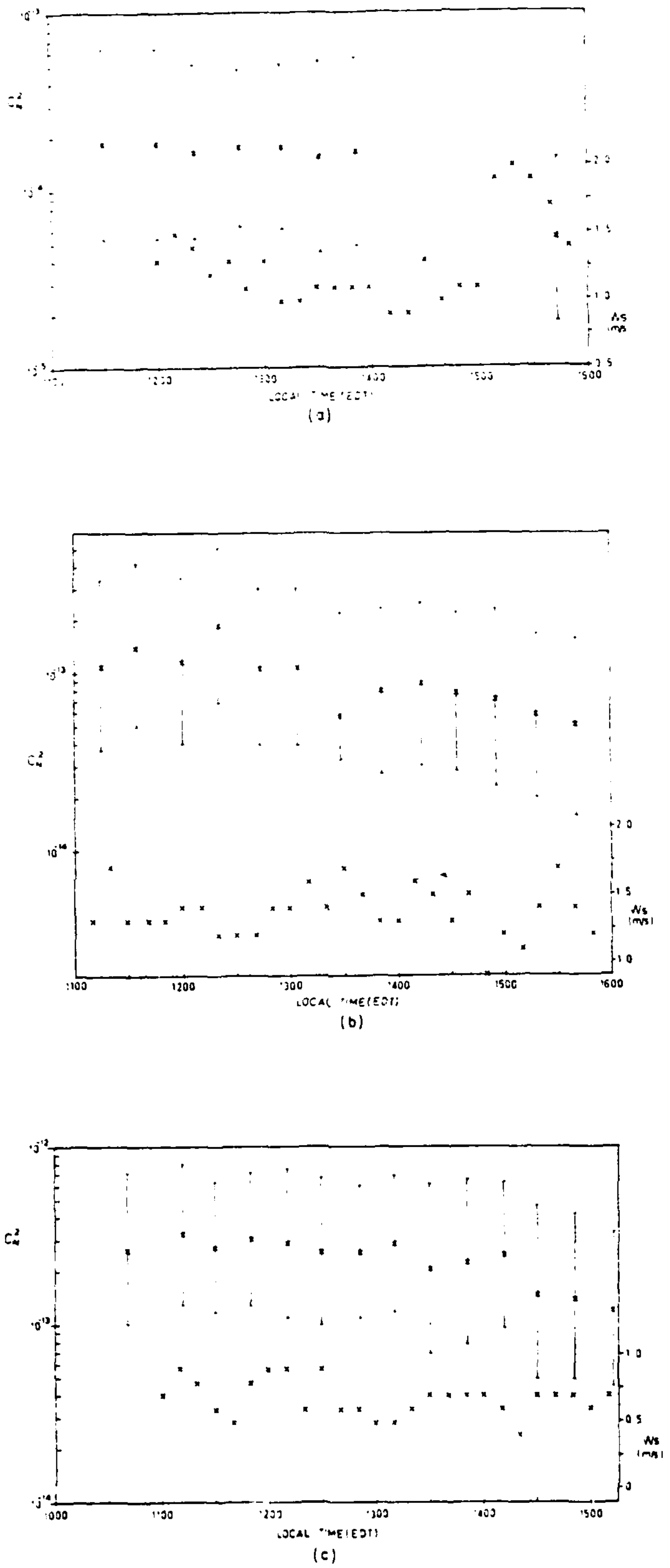

Fig. 15 — Average C_N^2 levels with standard deviation and wind speed measured at cliff top on (a) June 17 (b) June 22 and (c) June 23 1983

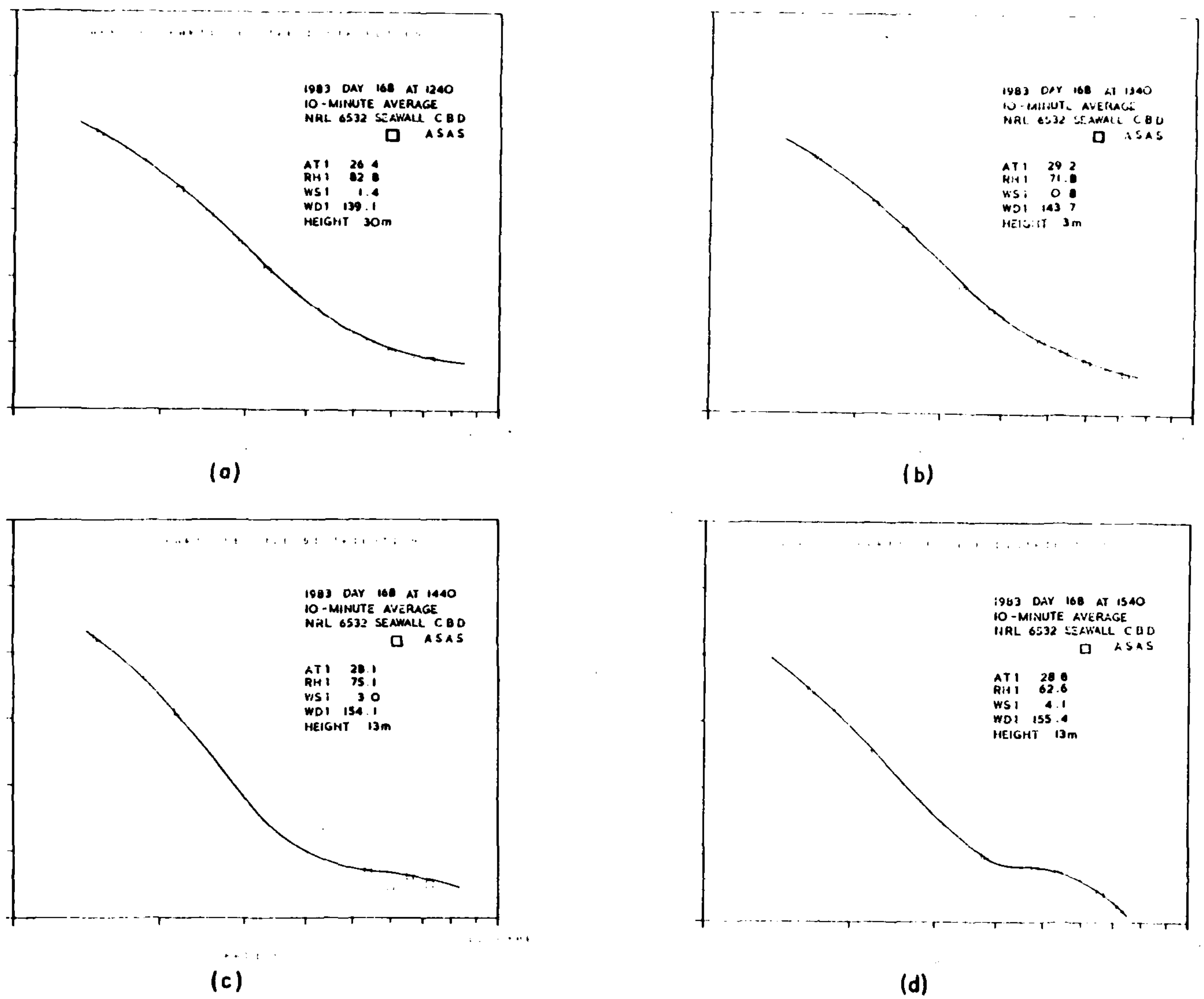

Fig. 16 — DN/DR versus radius on June 17 1983 for (a) 1230 to 1240, (b) 1330 to 1340, (c) 1430 to 1440 and (d) 1530 to 1540 EDT

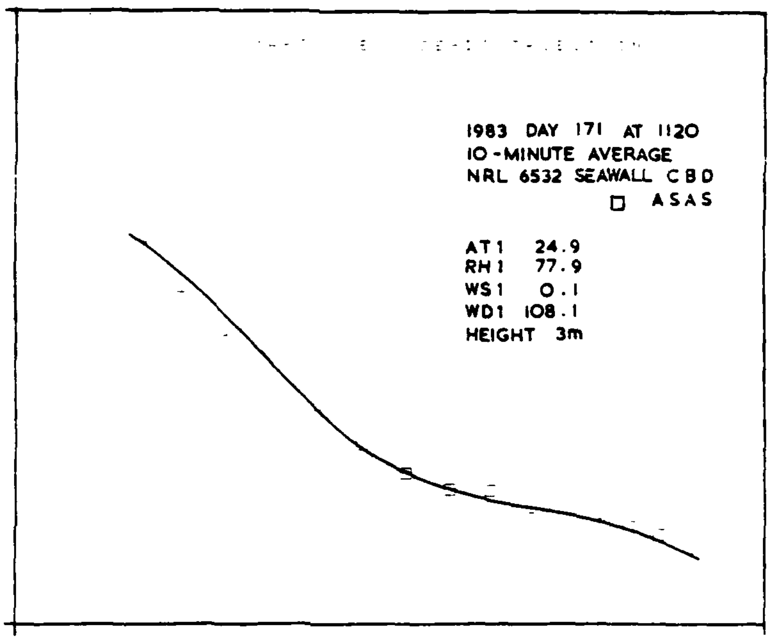

(a)

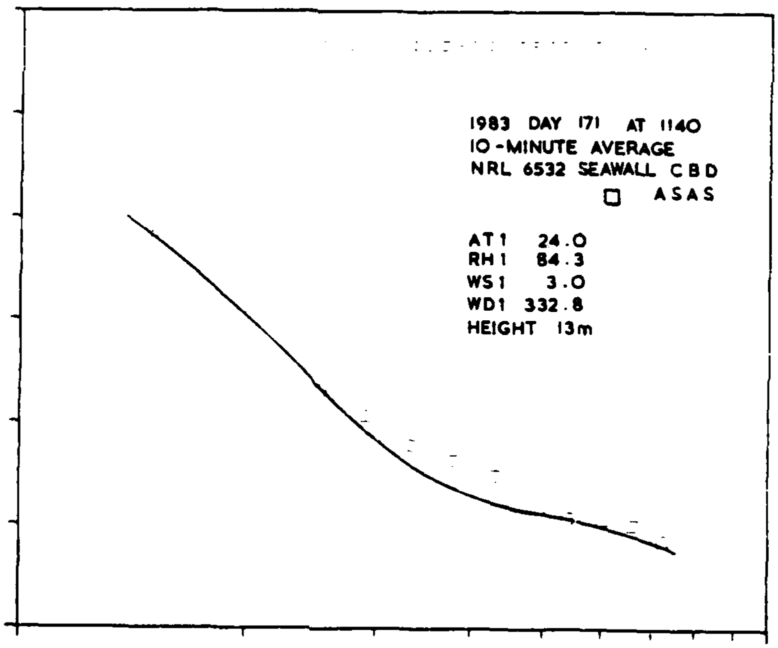

(b)

Fig. 17 — DN/DR versus radius on June 21 1983 for (a) 1110 to 1220 and (b) 1130 to 1140 EDT

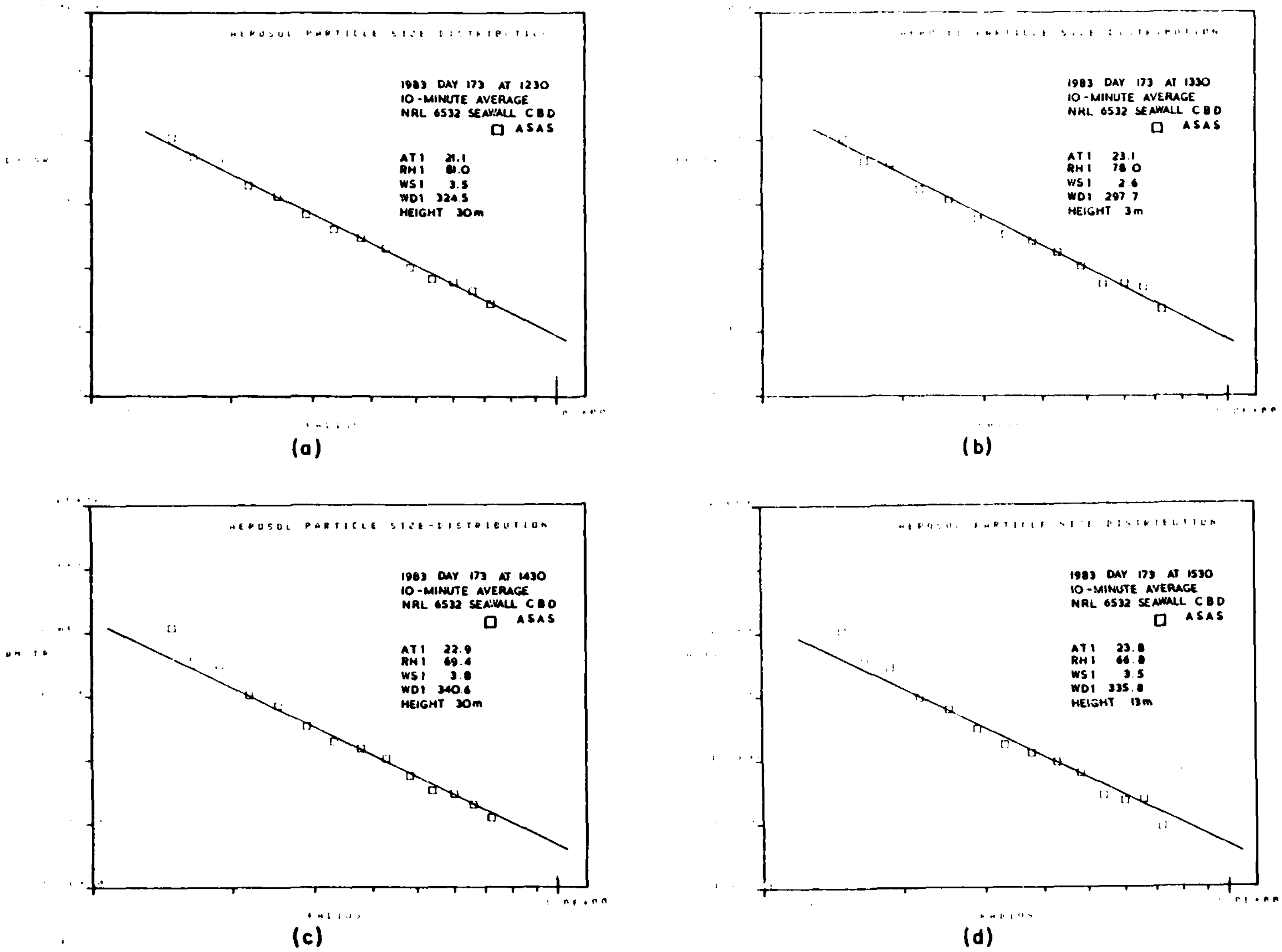

Fig. 18 — DN/DR versus radius on June 23 1983 for (a) 1120 to 1230, (b) 1320 to 1330, (c) 1420 to 1430 and (d) 1520 to 1530 EDT

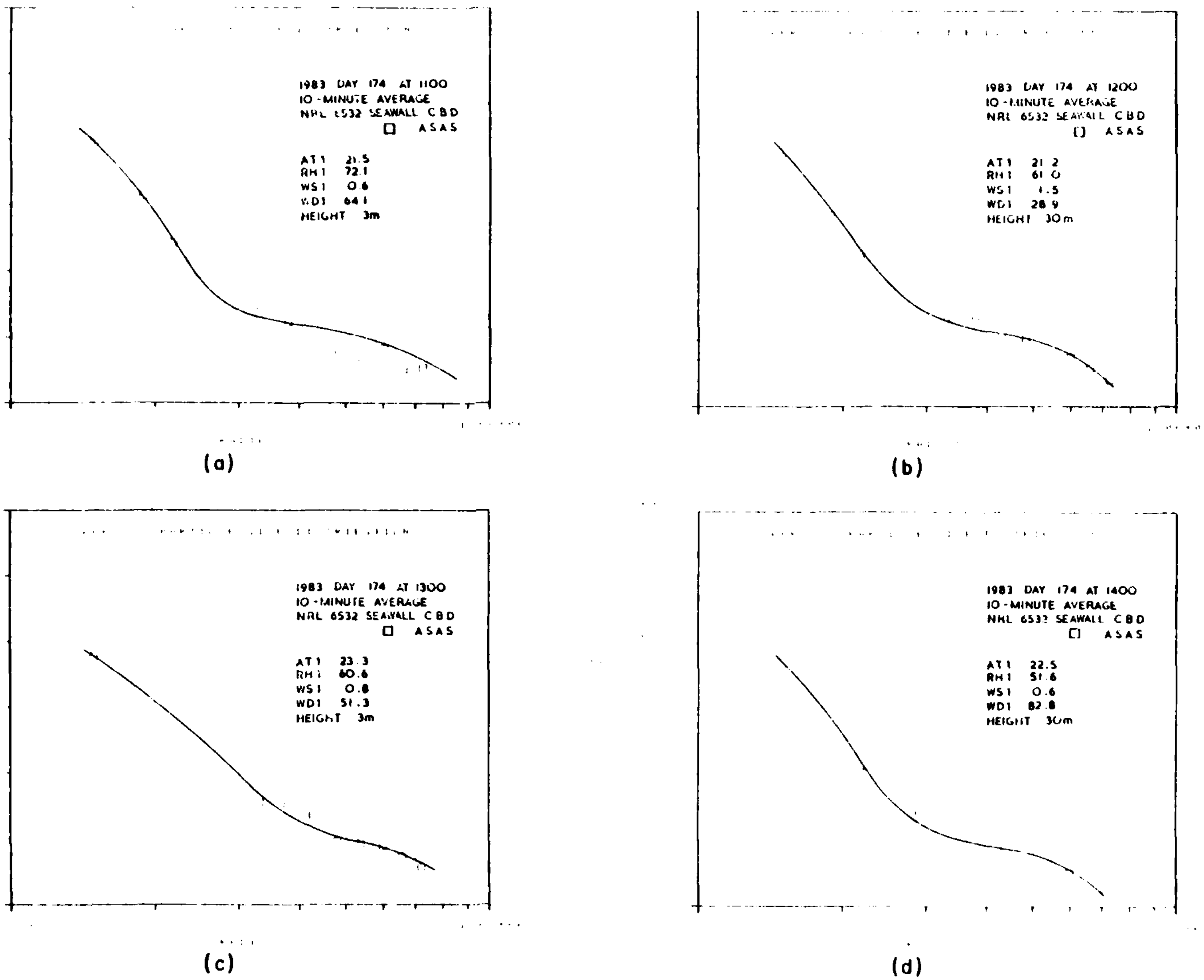

Fig. 19 — DN/DR versus radius on June 23 1983 for (a) 1050 to 1100, (b) 1150 to 1200, (c) 1250 to 1300 and (d) 1350 to 1400 EDT

REFERENCES

No.	Author	Title
1	Cutten, D.R.	"Measurements of Optical Turbulence Parameters Aboard the Aircraft Carrier USS LEXINGTON". NRL Memorandum Report 4911, September 30, 1982 (AD-A120 169)
2	Trusty, G.L. and Haught, K.M.	"An Aerosol Data Base Format". NRL Memorandum 4605, September 24, 1981 (AD-A107 032)
3	Wyngaard, J.C., Izumi, Y. and Collins, J.A., Jr.	"Behaviour of the Refractive-Index Structure Parameter near the Ground". JOSA Vol.61, page 1646, 1971
4	McCullough, D., Hines, J., Kunkel, K. and Hoidale, G.	"Atmospheric Conditions at the High Energy Laser Systems Test Facility (HELSTF) White Sands Missile Range, New Mexico, 16 to 18 October 1979". ASL-DR-80-0008, December 1980 (AD-B063 069)
5	Kneizys, F.X. et al	"Atmospheric Transmittance/Radiance: Computer Code LOWTRAN 5". AFGL-TR-80-0067, 1980 (AD-A088 215)